

# Lasers and Space: remediation of the dangerous and unavoidable [1-10] cm debris. Mini-Euso on ISS: a demonstrator

Philippe Gorodetzky, APC, Paris, France

Toshi Ebisuzaki, Riken, Wako, Japan

Marco Casolino, Riken, Wako, Japan

Marco Ricci, Tor Vergata, Rome, Italy

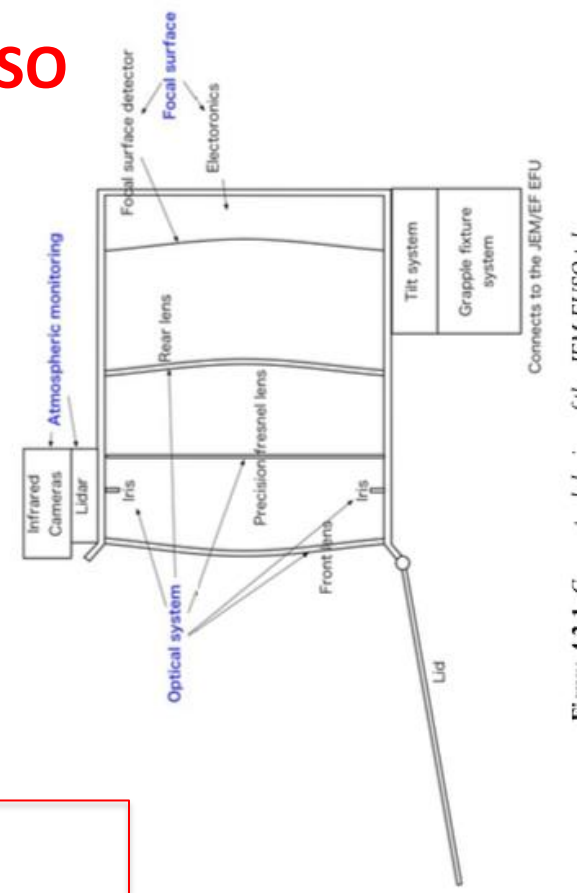
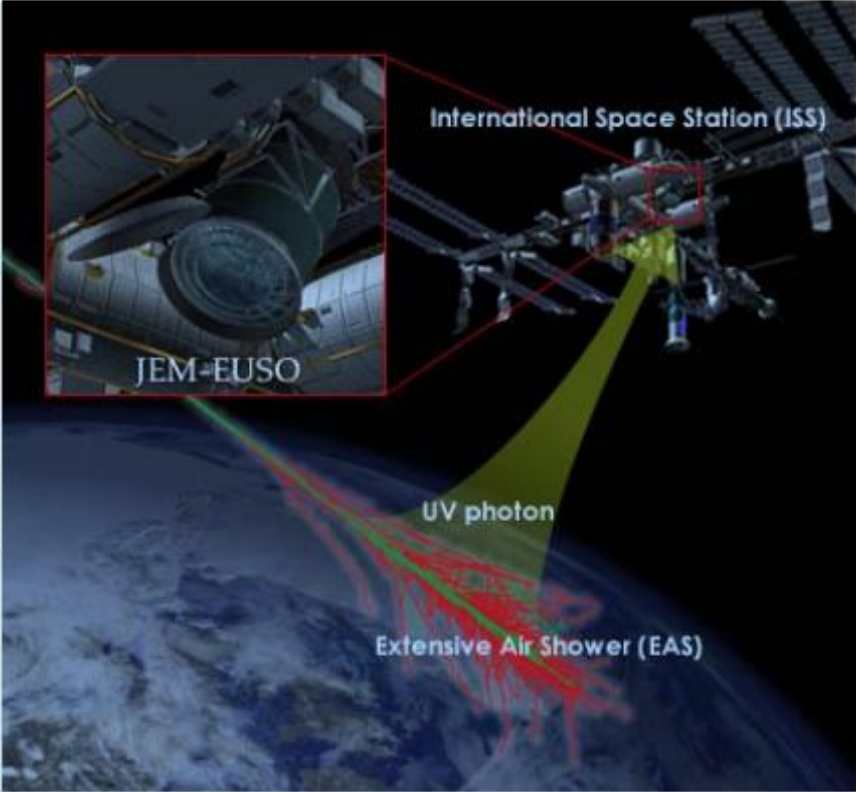
+ ...

IZEST conference

**Outlook on Wakefield Acceleration: the Next Frontier**

CERN, Geneva, Switzerland, October 15 & 16

# JEM-EUSO



**Focal Surface detector**

**Elementary Cell  
(2x2 PMTs = 144 pixels)**

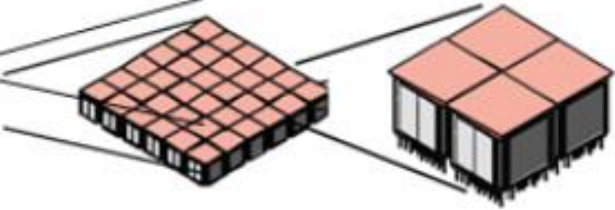
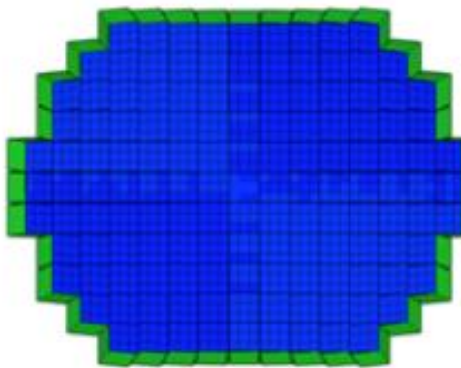
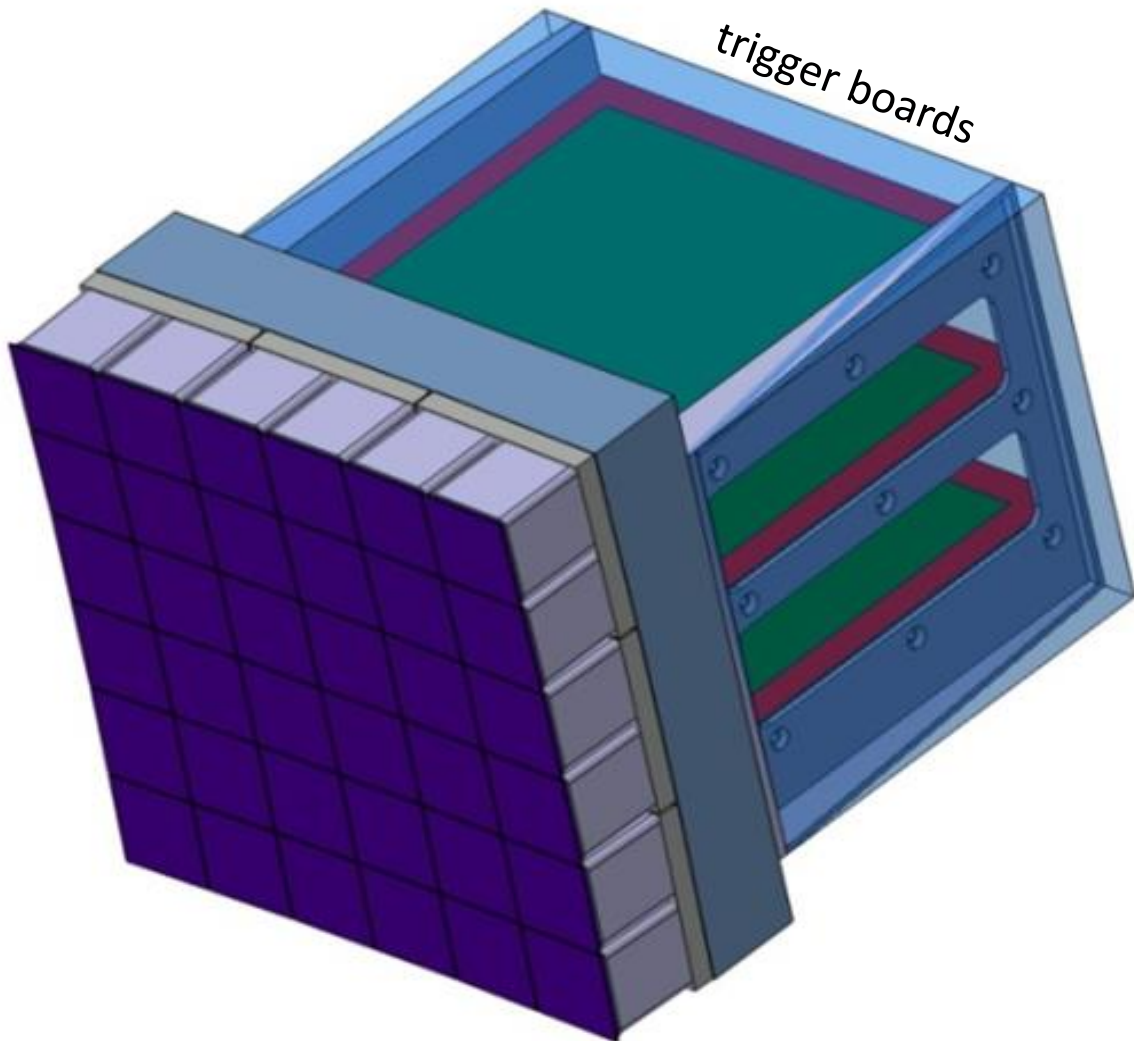


**Photo-Detector Module  
(3x3 ECs = 1296 pixels)**

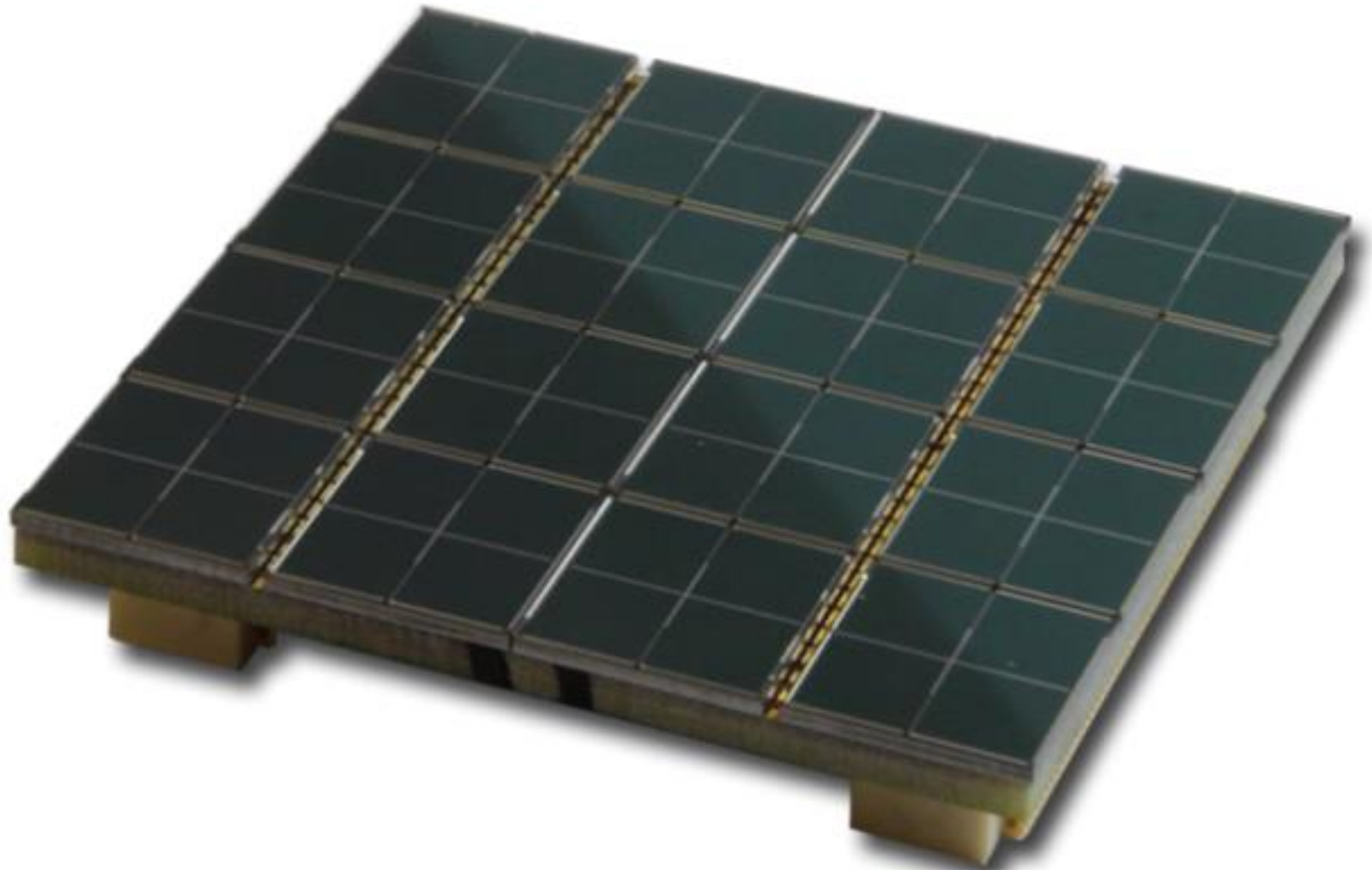
The photon detector module (PDM): 6 x 6 PMT (in blue, because covered by BG3 filters, [300-400 nm]), each having 64 pixels (total 2304 pixels of 2.88 x 2.88 mm). 4 PMTs could be replaced by SiPM, without filters.

Each dynode has its own high voltage power supply, located in the PMT socket (very low power consumption and very low impedance: large dynamics). HV is potted.



In green, the front end ASICs, 64 channels each, based on a discriminator (5 ns) per channel, to work in "photon counting" mode. The integration time is basically 2.5  $\mu$ s, during which up to 140 photoelectrons (pe) can be counted individually before pile-up appears. When the number of pe is > 100, a high voltage switch lowers the cathode voltages, leaving all other dynodes untouched. This only destroys the collection efficiency. Single pe mode is kept. The dynamics, this way, can reach  $10^6$ .

# TEST OF ADVANCED INSTRUMENTATION: SiPM



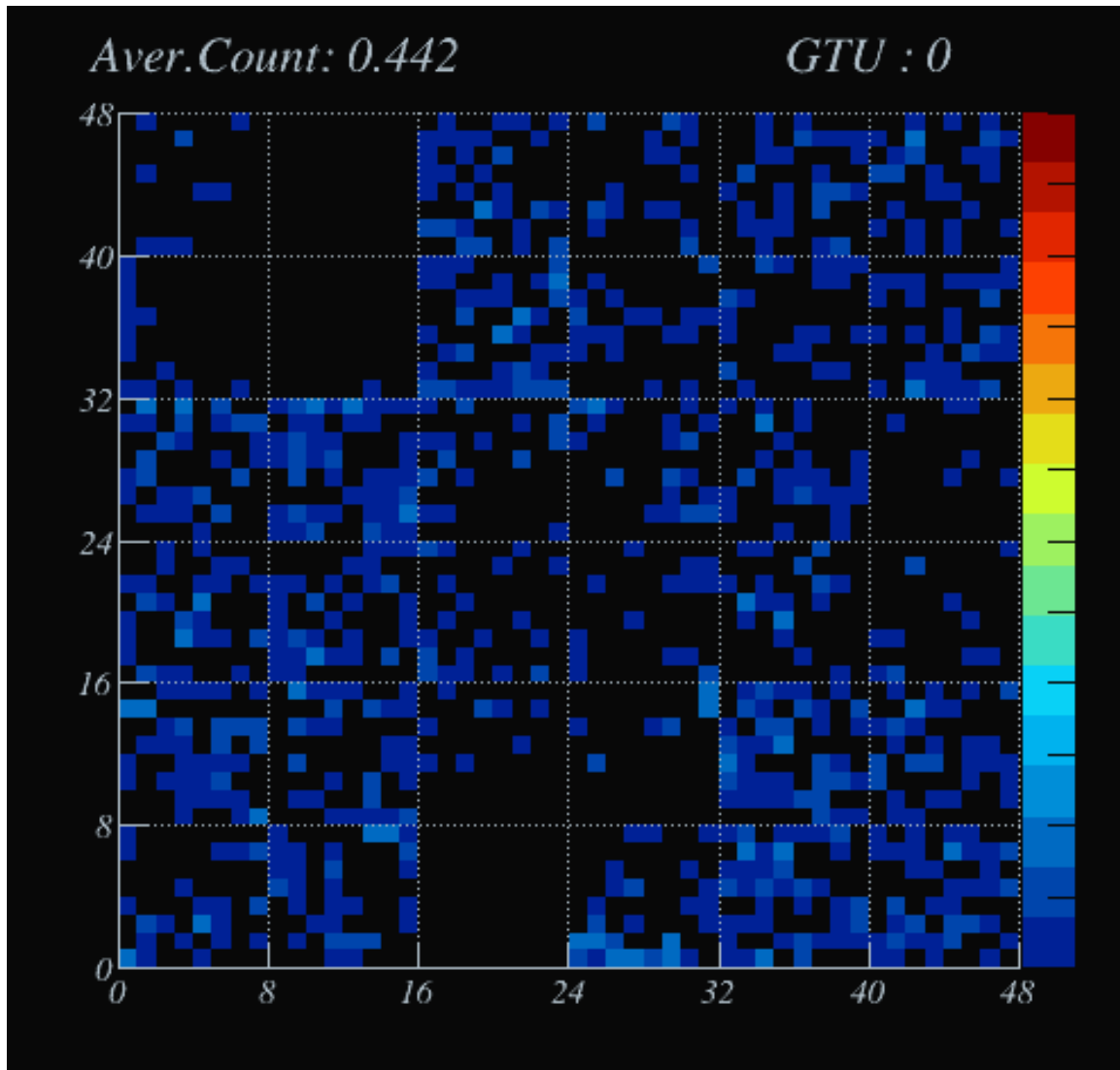
We will have one EC (5 x 5 cm) of SiPM installed with their electronics next to to the PMTs



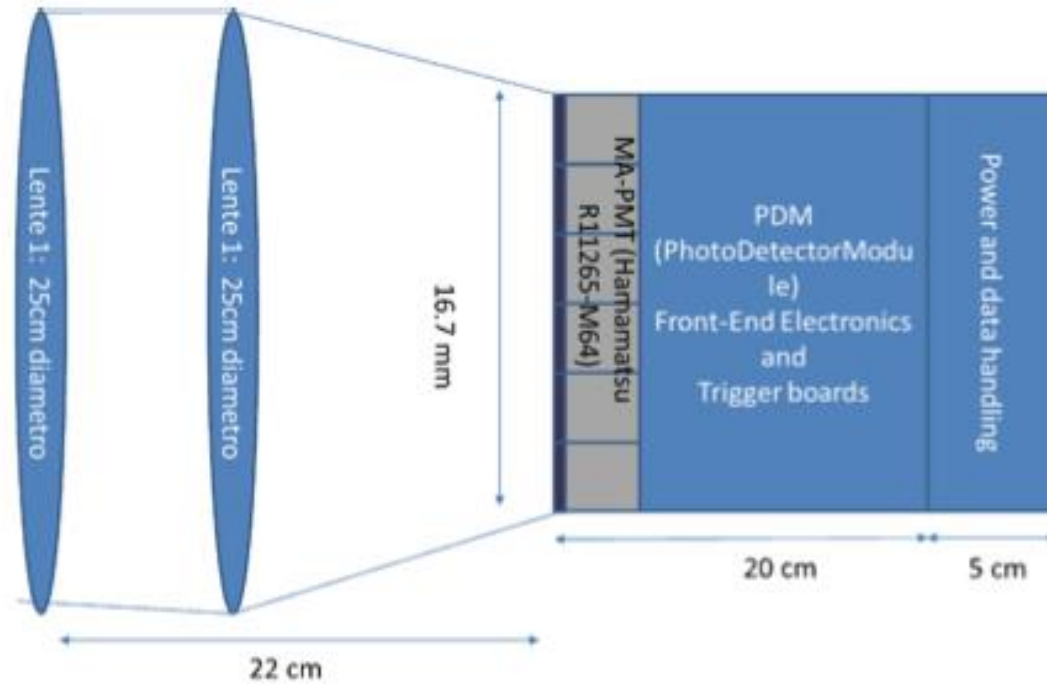
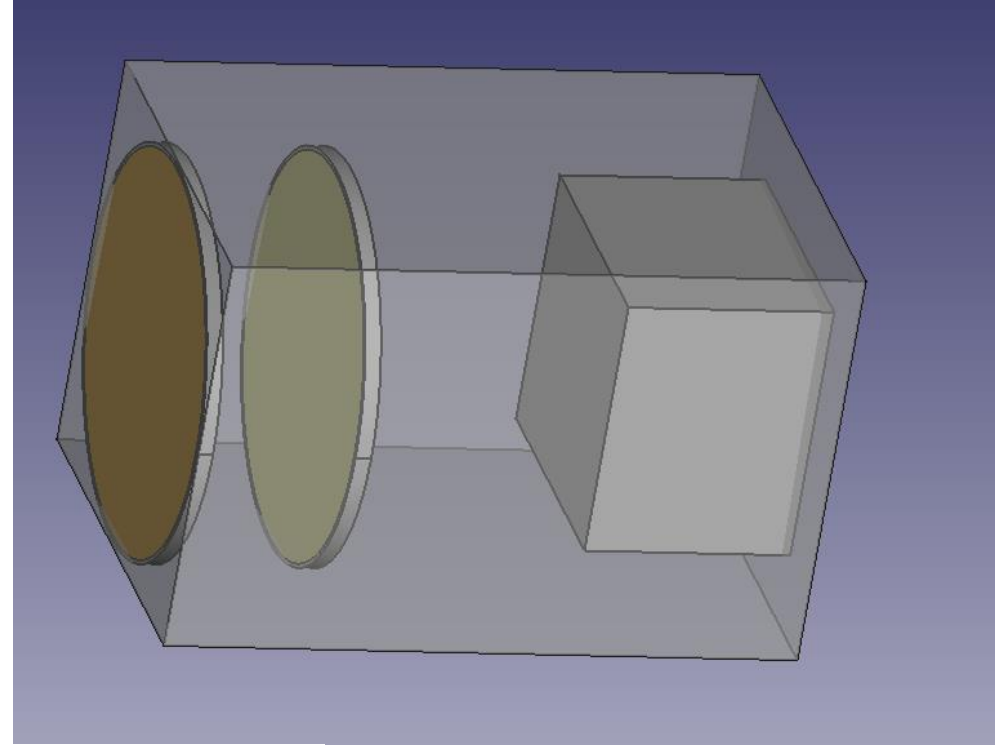
One PDM flew in this balloon from Timmins (Canada) in June 2014.



ÉTUDE DU FONCTIONNEMENT  
D'UN TÉLESCOPE DE  
FLUORESCENCE DANS LE  
CADRE DU PROJET EUSO-  
BALLOON



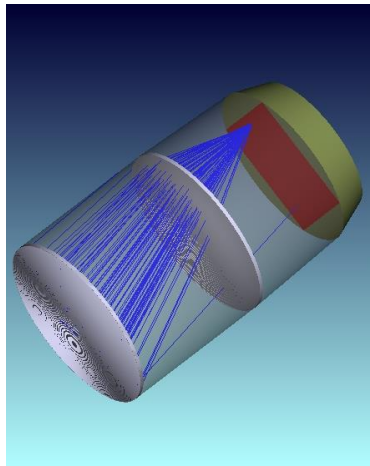
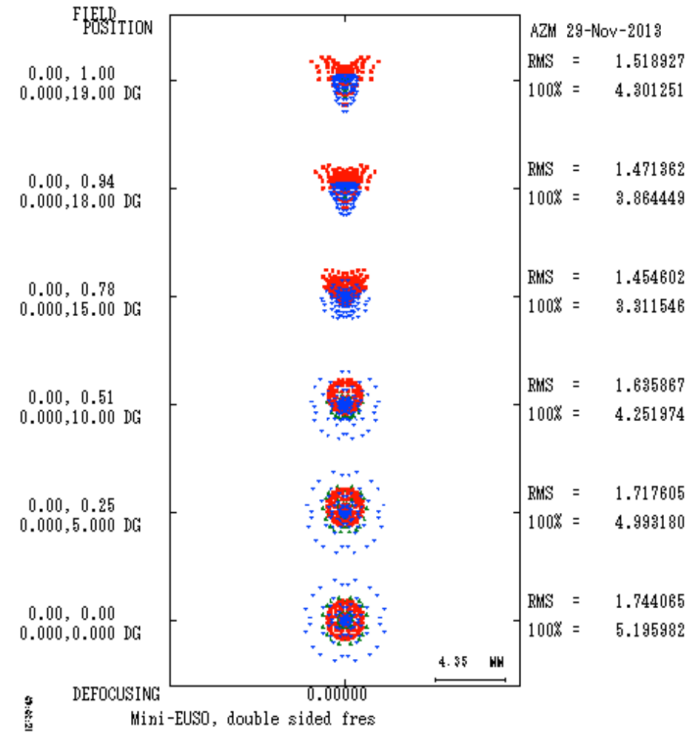
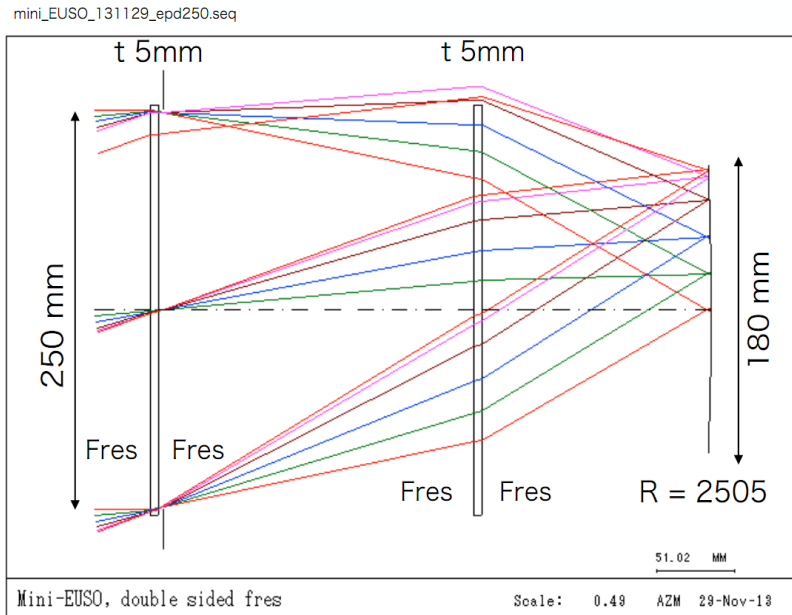
# Conceptual scheme of mini-EUSO



# Mini-EUSO design ver1

2013.11.29

Flat double sided fresnel lens x 2





# Scientific Objectives approved by ROSCOSMOS & ASI

- ***a) Scientific objectives***
- ***a.1) UV emissions from night-Earth***
  - 6.5 km resolution, from 2.5mus and above  $\pm 51^\circ$*
  - Noise from different lightning conditions, moon phase*
  - Noise from different inclinations*
- ***a.2) Map of the Earth in UV***
- ***a.3) Study of atmospheric phenomena***
- ***a.4) Bioluminescence of Animal and vegetal organisms***
- ***a.4) Study of meteors***
  - *Search for Strange quark matter*
  - *Space Debris assessment*

**Project was approved by ASI October 2<sup>nd</sup> to be launched in May 2017.  
Italian astronaut Paolo Nespoli will conduct locally the experiment**

# Monitoring of the UV background

The knowledge of the UV background is essential to understand:

- a) energy threshold of a space-based mission
- b) exposure as it is related to the duty cycle

In the performance papers (Astroparticle Physics, Advances in Space Research, and Experimental Astronomy) we based our considerations on Balloon experiments and models without using satellite data results in the UV band for the following reasons:

- a) Tatiana 1 and Tatiana 2 had very large FoV on a single pixel (order of 100 km radius) which can give different responses on limited illuminated area (ex. cities)
- b) We understood that Tatiana 1 from time to time was not pointing to the Earth (we have no idea when)
- c) Tatiana 2 operated only for 2-3 months

Moreover:

- d) EUSO-Balloon can not tell us the role of the Airglow at 100 km altitude

# Mini-Euso will tell us:

- a) Which is the average UV-background level seen from the ISS on a pixel size level of  $\sim 5 \times 5 \text{ km}^2$
- b) How variable is the UV background spatially and temporally (we know from our Slovakian colleagues using AURIC model that background is variable!)
- c) Which is the reduction of the duty cycle due to presence of city or any other artificial light, as well as due to lightning or any other natural phenomena.
- d) Which is the impact of the South Atlantic Anomaly (can we operate or not?).

All the above will be measured exactly in the conditions in which KLYPVE/JEM-EUSO are expected to operate: ISS orbits!!!

# TECHNOLOGICAL ASPECTS

- a) First use of Fresnel Lenses in Space (meant as higher than the edge of atmosphere like 40 km altitude)
- b) Optimization and Validation of JEM-EUSO observational scheme
- c) Increase of readiness level of JEM-EUSO instrumentation
- d) Test of advanced solutions for future space missions, such as SiPM in view of S-EUSO like telescopes

# OTHER SCIENTIFIC ITEMS

- a) albedo measurements
- b) meteor studies
- c) Airglow Gravity Waves
- d) Transient Luminous Events
- e) Strange Quark Matter



# ALBEDO MEASUREMENTS

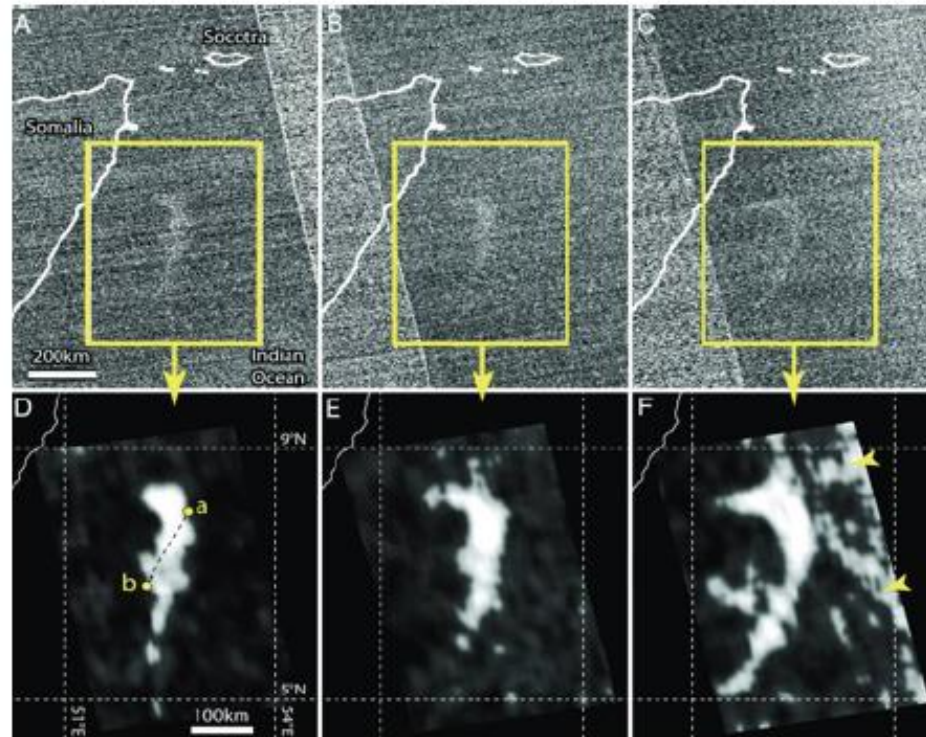
- a) MINI-EUSO will test the Poissonian behaviour of background fluctuations at  $\mu\text{s}$  level.
- b) MINI-EUSO will measure the albedo in different conditions: ocean, desert, snow/ice, lakes, forests, clouds, etc... Part of these values will be soon known from EUSO-Balloon flight, but we will see the effect of the airglow (different from EUSO-Balloon)
- c) MINI-EUSO will check the reflection of the Moon from Earth on different surfaces, understanding with which uncertainty the moon light could be used for absolute calibration

# BIO-LUMINESCENCE PHENOMENA

Bioluminescence – only one (?) confirmed observation of “milky sea” from space

Known spectra rather in visual range

UV-sensitive organisms known – possibility of undiscovered UV bioluminescence



# METEOR STUDIES

MINI-EUSO covers a FoV at ground of about 300x300 km<sup>2</sup> therefore it is only **3-4** times smaller than JEM-EUSO and could be used to make a study of the meteor rate as a function of magnitude.

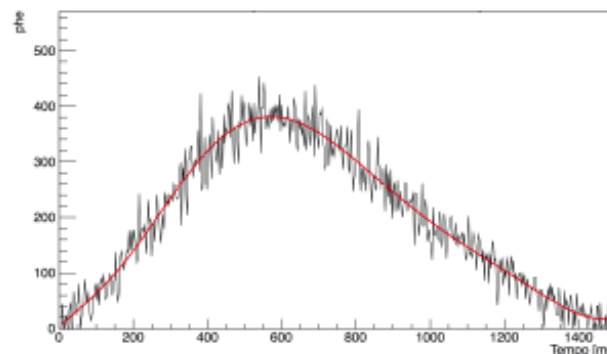
JEM-EUSO/K-EUSO will most probably operate as meteor detector only for limited time. MINI-EUSO, as it has no cosmic ray purposes, could spend much more time detecting these types of events.

The shape and light profile of these events as seen by MINI-EUSO will help the design of the trigger strategy for any future mission like K-EUSO or JEM-EUSO.

Comparing JEM-EUSO and MINI-EUSO, the signal in MINI-EUSO is **100 times** smaller due to the 10 times smaller lenses while the background level is kept constant because the pixel FoV is the same. Therefore, in principle,  **$\Delta M = +5$**  compared to JEM-EUSO. However, if the signal in JEM-EUSO is not fully contained in one pixel the S/N ratio will slightly improve.

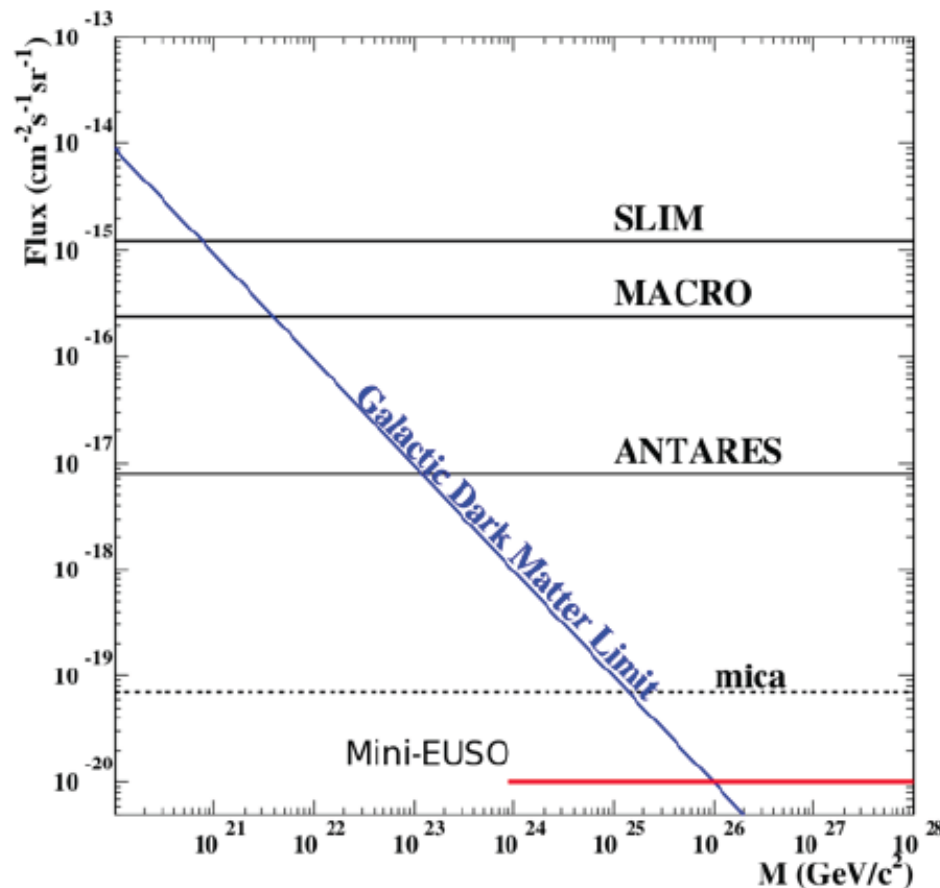
**The performance of MINI-EUSO for meteors is highly dependent on the possibility to have charge integration compared to photon-counting which limits the  $\Delta M = 4-5$ .**

**M=+2 in JEM-EUSO**  
**M=-3 in MINI-EUSO**



# STRANGE QUARK MATTER SEARCHES

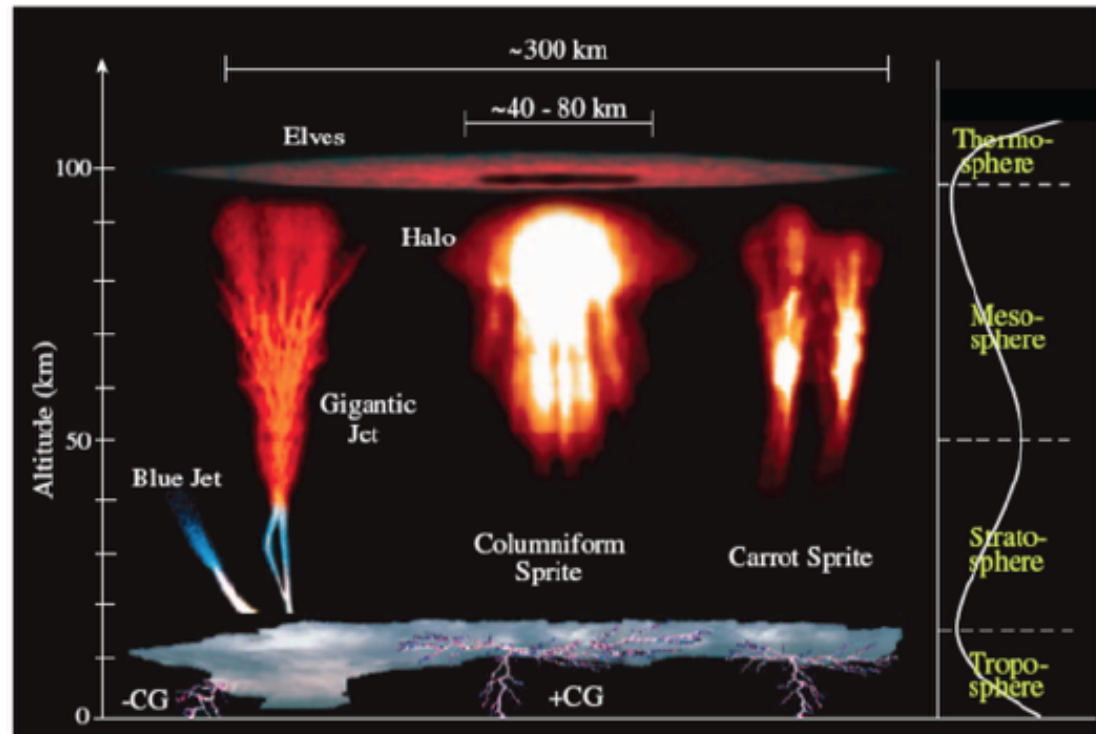
Nuclearites are characterised by light speed only 1 order of magnitude higher than meteors (270 - 540 km/s) therefore, the same principle used to detect meteors could be applied for Nuclearites as well.





# TRANSIENT LUMINOUS EVENTS

MINI-EUSO with high temporal and moderate spatial characteristics could monitor the rate of TLEs and the characteristics of their light curve in the early phases of the development with high accuracy.





# AIRGLOW GRAVITY WAVES & TSUNAMI WATCHER

## Atmospheric Gravity Waves model

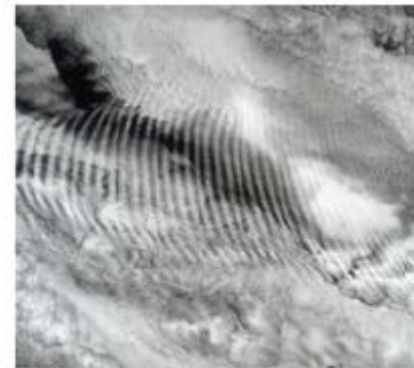
## Atmospheric Gravity Waves model

P. Bobik ([bobik@saske.sk](mailto:bobik@saske.sk)), M. Putiš, Š. Mackovjak

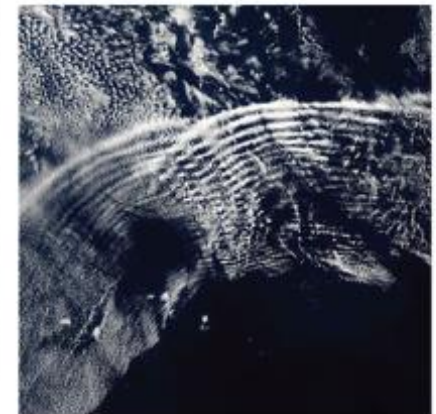
Institute of Experimental Physics, SAS



JEM-EUSO simulation and atmospheric meeting  
Toulouse, 1. October 2014



NASA, MODIS (Moderate Resolution Imaging Spectroradiometer)



### Background : Observation

#### Imaging and modeling the ionospheric airglow response over Hawaii to the tsunami generated by the Tohoku earthquake of 11 March 2011

J. J. Makela,<sup>1</sup> P. Legros,<sup>2</sup> H. Höbert,<sup>1</sup> T. Getrels,<sup>1</sup> L. Rolland,<sup>2</sup> S. Algeyer,<sup>3</sup> A. Kherani,<sup>4</sup> G. Occhipinti,<sup>2</sup> E. Artaforn,<sup>2</sup> P. Collinson,<sup>2</sup> A. Loewenbusch,<sup>2</sup> E. Clivade,<sup>2</sup> M. C. Kelley,<sup>2</sup> and J. Larroucous<sup>4</sup>

Received 19 April 2011; revised 27 May 2011; accepted 27 May 2011; published 7 July 2011.

[1] Although only centimeters in amplitude over the open ocean, tsunamis can generate appreciable wave amplitudes in the upper atmosphere, including the naturally occurring chemiluminescent airglow layer, due to the exponential decrease in density with altitude. Here, we present the first observation of the airglow tsunami signature, resulting from the 11 March 2011 Tohoku earthquake off the eastern coast of Japan. These images are taken using a wide-angle camera system located at the top of the Haleakala Volcano on Maui, Hawaii. They are correlated with GPS measurements of the total electron content from Hawaii GPS stations and the Jason-1 satellite. We find waves propagating in the airglow layer from the direction of the earthquake epicenter with a velocity that matches that of the ocean tsunami. The first ionospheric signature recorded that modeled ocean tsunami generated by the main shock by approximately one hour. These results demonstrate the utility of monitoring the Earth's airglow layer for tsunami detection and early warning. © 2011 The Authors. Journal of Geophysical Research. DOI: 10.1029/2011GL047860

Observation by highly sensitive, wide-angle camera system to image the tsunami-driver ionospheric response to the 11 March 2011 Tohoku earthquake.

From a single instrument located on the Haleakala Volcano on Maui, Hawaii, able to image a  $10^6 \text{ km}^2$  region of the ionosphere at high spatial (1–5 km, elevation angle dependent) and temporal (5 min) resolution

Observing the airglow layer at approximately 250 km in altitude caused by the dissociative recombination of  $\text{O}_2^+$  which emits photons at 830.0 nm.

J. J. Makela et al., Imaging and modeling the ionospheric airglow response over Hawaii to the tsunami generated by the Tohoku earthquake of 11 March 2011, GRL, VOL. 38, L00G02, doi:10.1029/2011GL047860, 2011

### Background : Observation

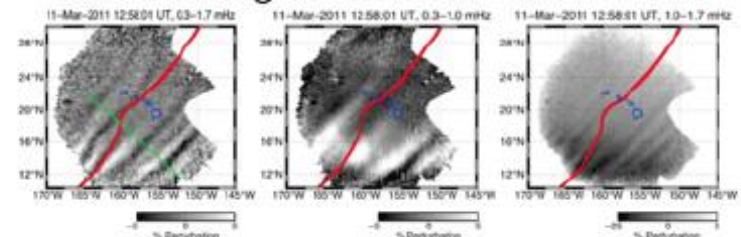


Figure 1. Example of 630.0-nm images processed using length-8 FIR filters with passbands of (left) 0.3–1.7 mHz, (middle) 1.0–1.7 mHz to highlight the 26.2-min period waves, and (right) 1.0–1.7 mHz to highlight the 14.2-min period waves. The red line in each image indicates the tsunami location at the time of the image. The green line in Figure 1 (left) indicates the line from which intensities were taken to construct Figure 2.

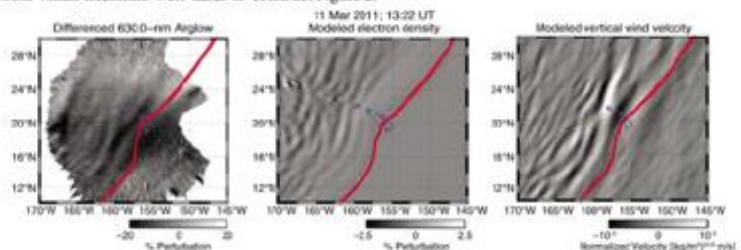


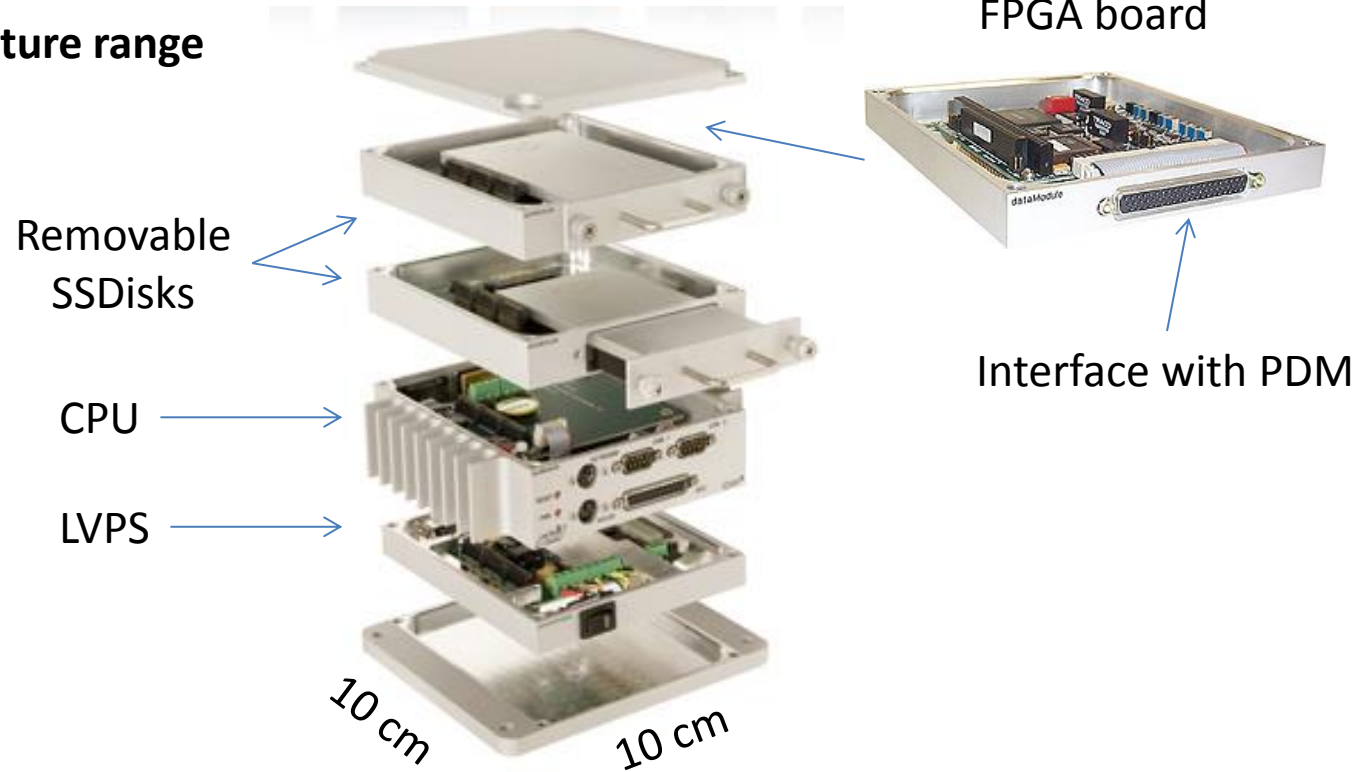
Figure 3. Comparison of (left) differenced 630.0-nm emission intensity observed at 13:20 and 13:22 UT from Hawaii, (middle) electron density at 250 km from a gravity-acoustic model [Kherani et al., 2009], and (right) normalized vertical wind velocity at 250 km from a pure gravity wave model [Occhipinti et al., 2006, 2008, submitted manuscript, 2011]. In each case, the red line indicates the tsunami location at the time of the image.

J. J. Makela et al., Imaging and modeling the ionospheric airglow response over Hawaii to the tsunami generated by the Tohoku earthquake of 11 March 2011, GRL, VOL. 38, L00G02, doi:10.1029/2011GL047860, 2011

# Mini Euso Data Acquisition System

PCIe/104 standard

-40 + 85°C temperature range



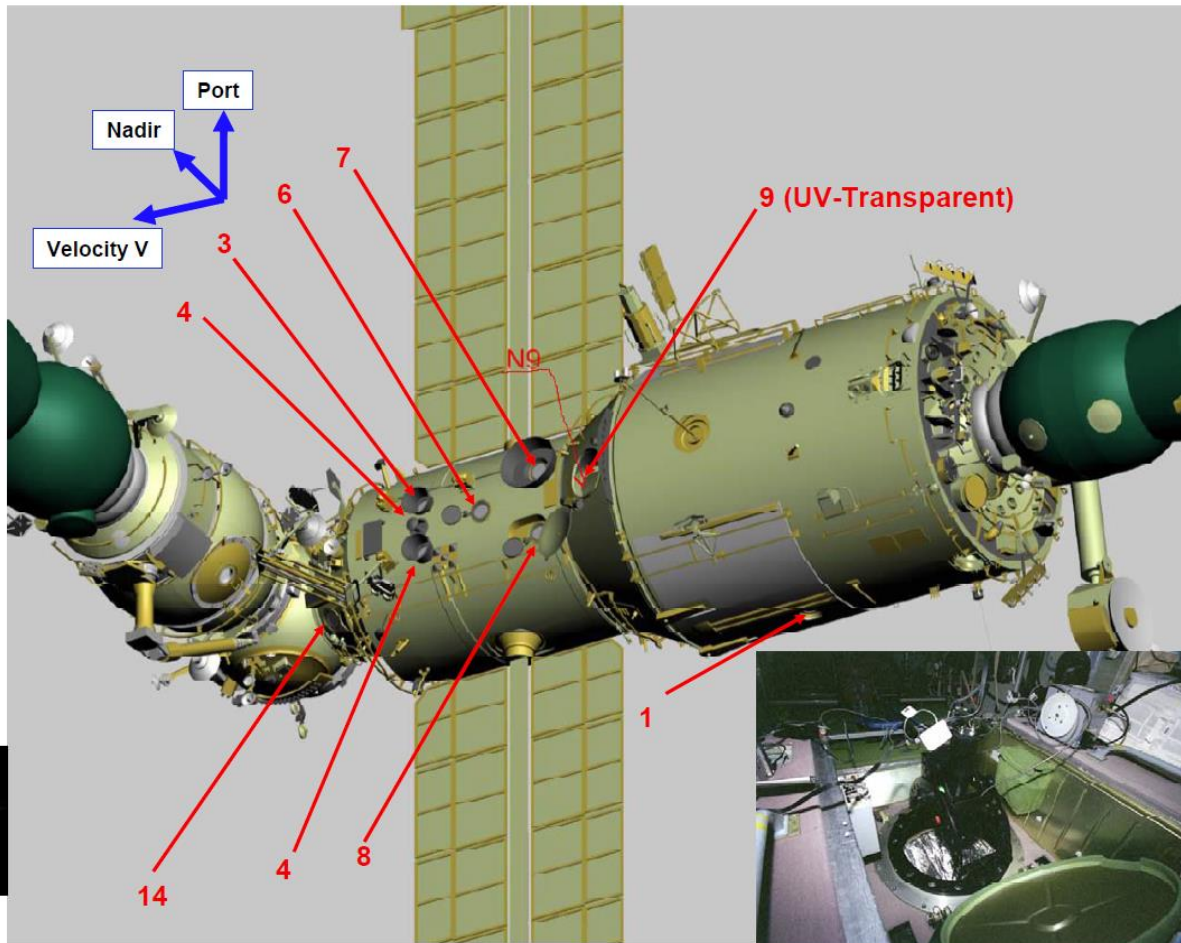
**CPU:** 1.20 GHz Single Core Intel® Celeron® M (ULV 722), 13 W, 3 SATA ports

**Mass memory:** several removable 512 GB Solid State Disks

From G. Osteria

Location: on Zvezda.

"9" is the 40 cm fused silica diameter window

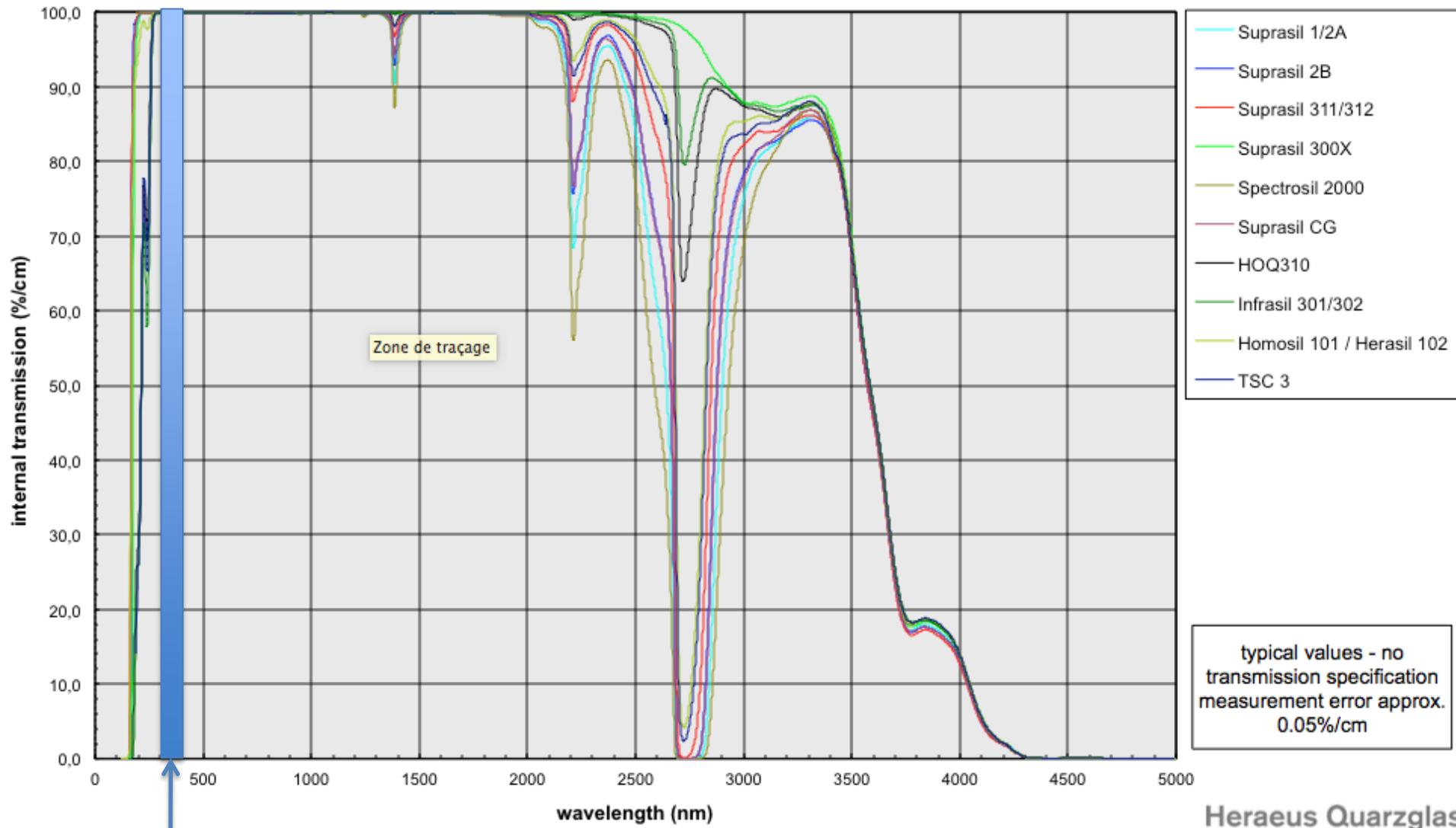




## Experiment "Relaxation" on the Zvezda widow



# Internal transmission excluding surface reflection losses

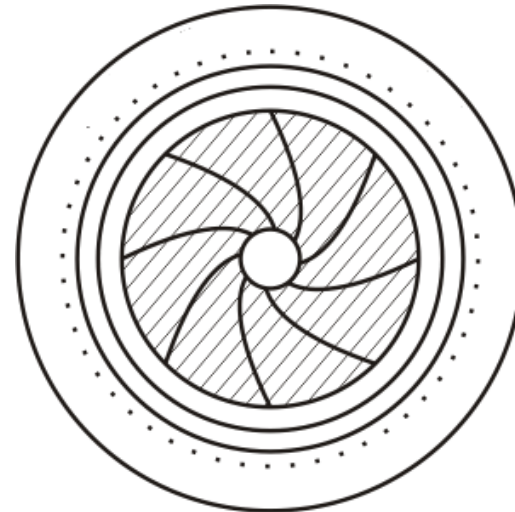
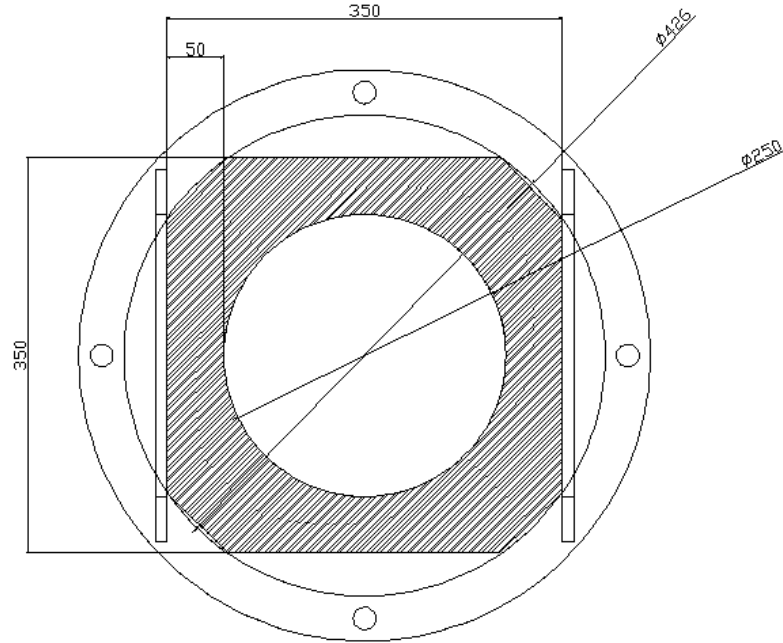
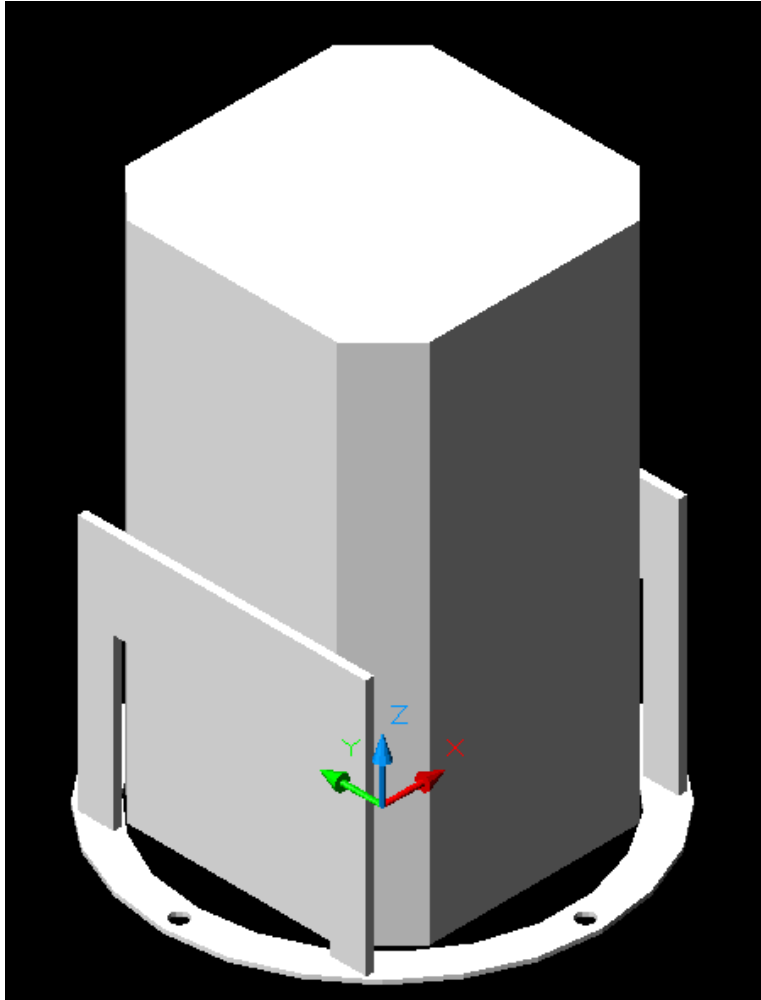


BG3 bandwidth

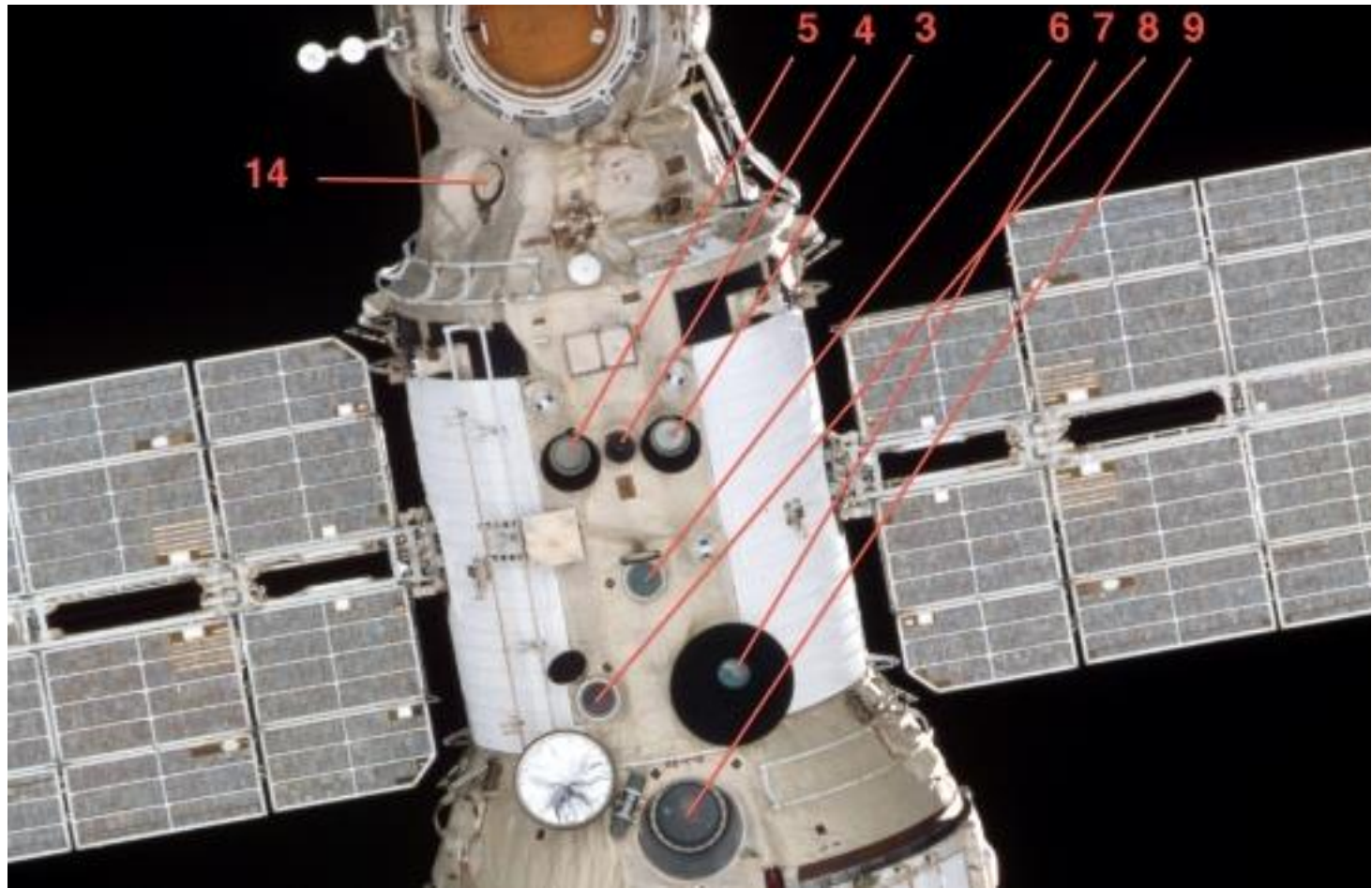
typical values - no transmission specification measurement error approx. 0.05%/cm



# 3D model of mechanical structure

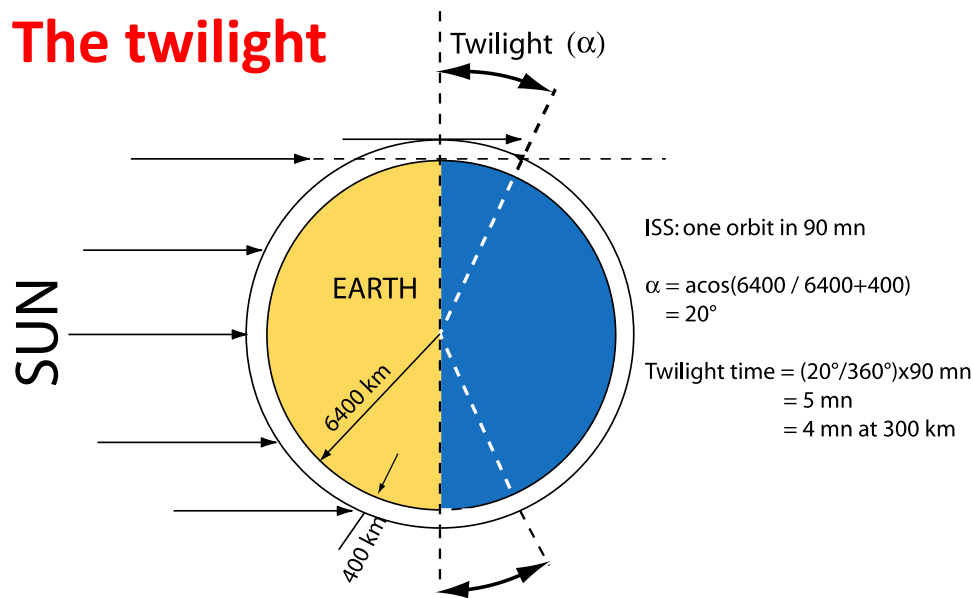


Diaphragm  
(protection  
against sun rays)

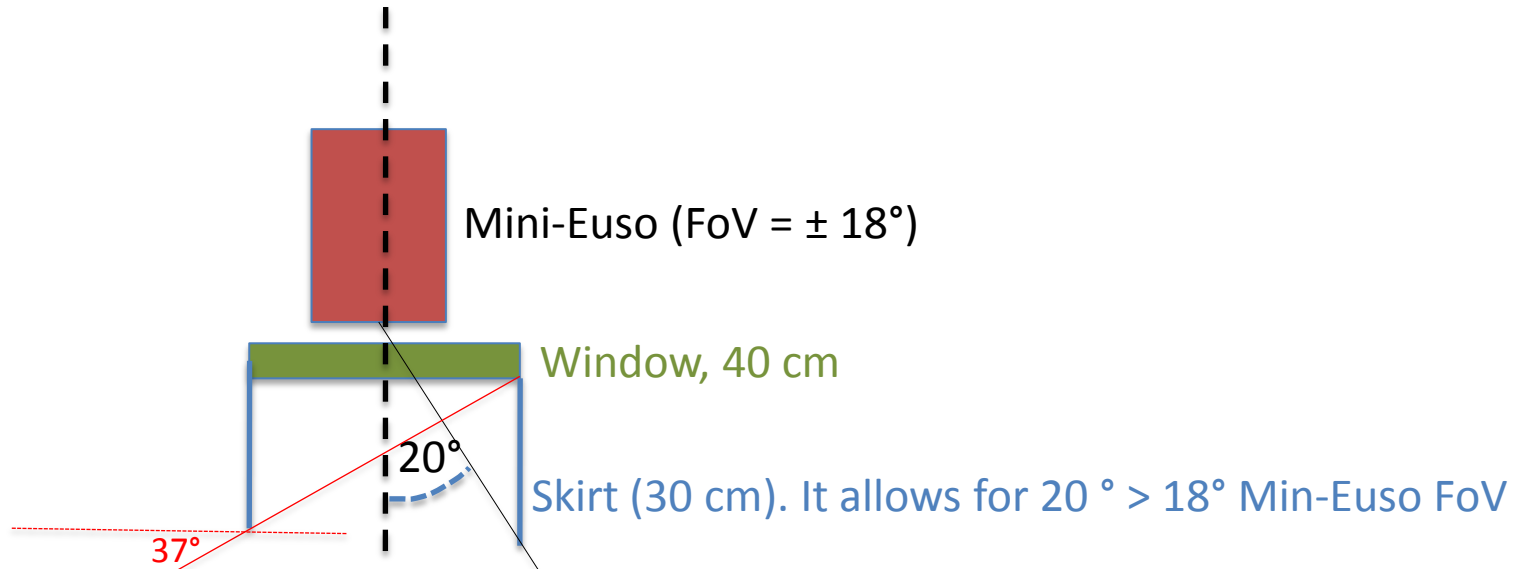


"9" (bottom) is the 40cm window. It looks there is a skirt which seems to extend some 30 cm. Important for debris assessment.

# The twilight



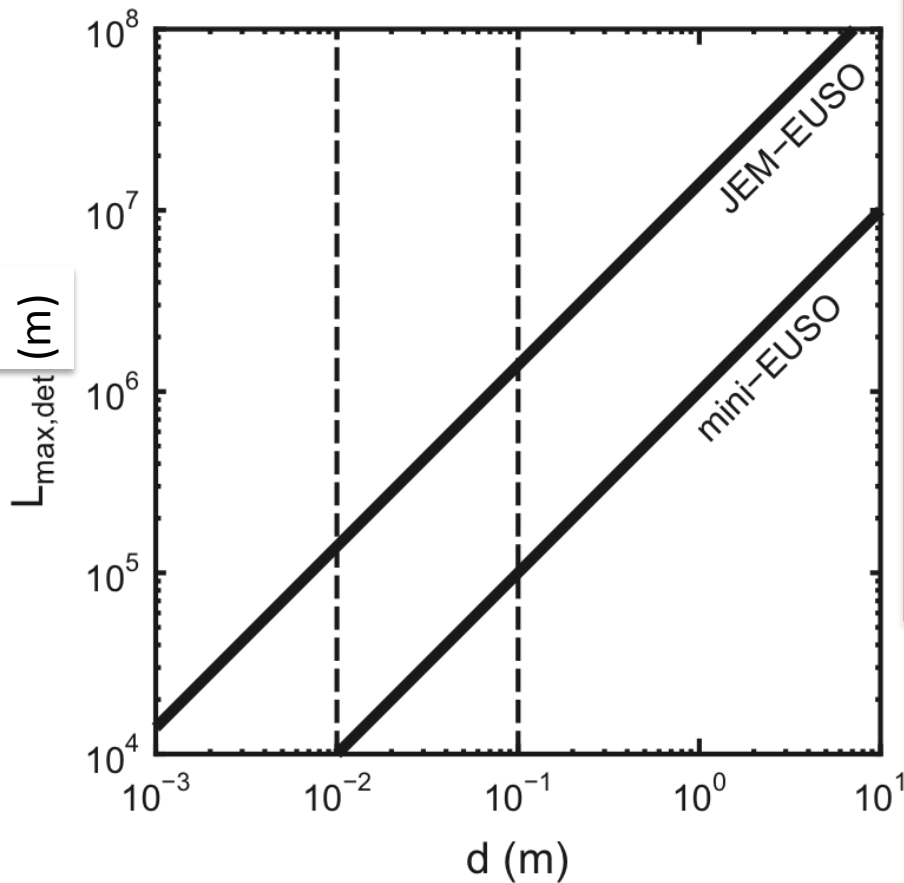
The ISS altitude is exaggerated to make the drawing easy to understand



Extreme sun ray:  $37^\circ$  with horizontal,  $\gg 20^\circ$  twilight angle

➔ no danger of sunlight through lenses

# Mini-Euso and the debris



Toshi's recent paper



Contents lists available at [ScienceDirect](https://www.sciencedirect.com)

Acta Astronautica

journal homepage: [www.elsevier.com/locate/actaastro](http://www.elsevier.com/locate/actaastro)

## Demonstration designs for the remediation of space debris from the International Space Station

Toshikazu Ebisuzaki<sup>a,\*</sup>, Mark N. Quinn<sup>b</sup>, Satoshi Wada<sup>a</sup>,  
Lech Wiktor Piotrowski<sup>a</sup>, Yoshiyuki Takizawa<sup>a</sup>, Marco Casolino<sup>a,c</sup>,  
Mario E. Bertaina<sup>c,d</sup>, Philippe Gorodetzky<sup>e</sup>, Etienne Parizot<sup>e</sup>,  
Toshiki Tajima<sup>b,f</sup>, Rémi Soulard<sup>b</sup>, Gérard Mourou<sup>b</sup>

<sup>a</sup> RIKEN, 2-1, Hirosawa, Wako 351-0198, Japan

<sup>b</sup> IZEST, Ecole Polytechnique, 91128 Palaiseau, France

<sup>c</sup> INFN, Structure of Rome Tor Vergata, Via della Ricerca Scientifica 1, Rome, Italy

<sup>d</sup> University of Torino, Via P. Giuria, 1 10125 Torino, Italy

<sup>e</sup> APC-CNRS/Paris7 University, 1 rue A. Domonet L. Duquet, 75013 Paris, France

<sup>f</sup> Department of Physics and Astron, University of California at Irvine, Irvine, CA 92697, United States

$$L_{\max, \text{det}} = 1.4 \times 10^5 \left( \frac{F_{\text{sun}}}{10^{20} \text{ photons m}^{-2} \text{ s}^{-1}} \right)^{\frac{1}{2}} \\ \times \left( \frac{\xi_E}{0.1} \right)^{\frac{1}{2}} \left( \frac{\zeta}{0.1} \right)^{\frac{1}{4}} \left( \frac{\Delta}{0.08^\circ} \right)^{-\frac{1}{2}} \left( \frac{D_E}{2.5 \text{ m}} \right)^{\frac{1}{2}} \\ \times \left( \frac{\tau_d}{1 \text{ s}} \right)^{\frac{1}{4}} \left( \frac{d}{0.01 \text{ m}} \right) \text{ m.}$$

Maximum operation distance:  $L_{\max, \text{det}}$  (m) vs debris size  $d$ (m) for mini-EUSO where  $D_E=0.25$  m,  $\Delta$  (ang. res.) =  $0.6^\circ$  and  $\tau_d$  (time necessary to find trajectory) = 0.1 s.

$\zeta$ = collection efficiency of telescope  
 $\xi$ = reflection coefficient of debris

# Flux of debris to be detected by mini-EUSO

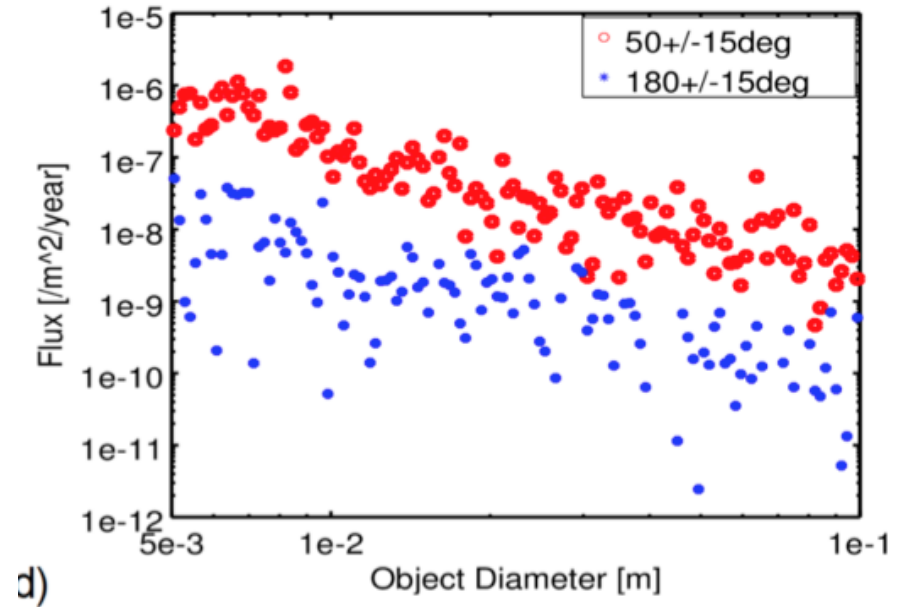
Number of photons emitted  
by debris lighted by sun:

$$F_{\text{debris}} = 3.1 \times 10^{15} \frac{F_{\text{sun}}}{10^{20} \text{ photons m}^{-2} \text{ s}^{-1}} \frac{X_E}{0.1} \frac{d}{0.01 \text{ m}}^2 \text{ photons s}^{-1}$$

Number of photons detected:  
with L distance to debris,, $D_E$  is  
telescope diameter and  $\zeta$  is  
the collection efficiency of the telescope

$$n_{\text{debris}} = \frac{\zeta N D_E^2 F_{\text{debris}}}{16 L^2}$$

Some 300 debris should pass the ISS within  
100 km per year.  
If we can measure for 2 x 5 mn every 90 mn



**we should detect 40 to 60 debris per year**

This is the first step of the demonstrator, before shooting at the debris.



Use of a ICAN prototype laser ( $\approx 100$  fibers) to shoot the debris.

The wavelength is 355 nm

The number of laser photons reflected by debris:

$$\begin{aligned}
 n_{laser} &= \frac{\chi z E_p N d^2 D^2}{\frac{hc}{c} \frac{1}{\theta} q^2 L^4} \\
 &= 1.0 \cdot 10^1 \frac{\chi}{0.1} \frac{z}{0.1} \frac{N}{10^2} \frac{E_p}{0.1 \text{ J}} \frac{1}{0.35 \text{ mm}} \\
 &\quad \cdot \frac{d}{0.03 \text{ m}} \frac{q}{0.01 \text{ rad}} \frac{L}{10 \text{ km}} \\
 &\quad \cdot \frac{D}{0.25 \text{ m}} \text{ photons}
 \end{aligned}$$

with  $\theta$  being the opening angle of the beam.

Here we are not limited by the twilight: we can use the 45 mn where the earth is dark.

In this demonstrator, we do not aim to slow down the debris, but to show that mini-Euso can detect it was hit by the laser.

It is expected we can hit about 10% of the detected debris

## CONCLUSION

Design parameters for testing debris remediation systems. Evolving initially onboard the ISS, the 'Prototype' provides testing of the key technologies in space and their operation in tandem, to be followed by a scaled-up 'Demonstrator' system to realise large distance delivery of pulses with sufficient fluence for  $\Delta v$  and directed propulsion. Once these systems have been proven reliable on the ISS, a free orbiting 'Dedicated' system can be considered for other more debris critical orbits such as near 800 km. For the latter 2 systems, laser focusing should be to the scale of the debris size at 100 km, with beam quality  $M^2 = 1$  and delivered pulse fluence  $\sim 10^4 \text{ Jm}^{-2}$ .

	Prototype at ISS orbit (400 km)	Demonstrator at ISS orbit (400 km)	Dedicated system near 800 km
Debris size (cm)	$> 1$	$10 > d > 0.5$	$10 > d > 0.5$
Debris distance (km)	$\sim 100$	$\sim 100$	$\sim 100$
Detector aperture	0.25 m	2.5 m	2.5 m
Photon detector (detection)	MAPMT	MAPMT	MAPMT
Wavelength (nm)	350–400	350–400	350–400
Angular resolution ( $^\circ$ )	0.8	0.08	0.08
Time resolution ( $\mu\text{s}$ )	2.5	2.5	2.5
Field of view	$\pm 14^\circ$	$\pm 30^\circ$	$\pm 30^\circ$
Background (photons/ms)	300	300	300
Pixel crossing time (ms)	10	1.2	1.2
$S/\sqrt{N}$ ratio	600	60	60
Laser focusing optics	0.25 m	1.5 m	1.5 m
Laser wavelength (nm)	335	355	355
Photon detector (tracking)	SiPM	SiPM	SiPM
Field of view ( $^\circ$ )	1.2	0.6	0.6
Spatial resolution ( $\mu\text{ rad}$ )	10	0.3	0.3
Number of pixels	$200 \times 200$	$1600 \times 1600$	$1600 \times 1600$
Response time (s)	0.01	3	3
Time resolution (ns)	1	1	1
Pulse energy (J)	0.1	1	1
Laser system	$10^2$ Fibres	$10^4$ Fibres	$10^4$ Fibres
Pulse energy (J)	0.1	10	10
Pulse duration (ns)	1	0.1	0.1
Repetition rate (Hz)	$10^2$	$10^4$	$5 \times 10^4$
Laser average power (W)	10	$10^5$	$5 \times 10^5$
Events per year	20–30 (detection) 2–3 irradiation)	10 (backward) 300 (forward)	$1.6 \times 10^5$ (forward) $1.6 \times 10^3$ (backward)

Mini-Euso is to be launched in May 2017 with, hopefully, an ICAN laser.